Short Communication

A Novel Enzyme-Free Glucose Sensor Based on Nickel Molybdate Nanosheets

Zhi Cao, Daojun Zhang, Chunying Xu, Renchun Zhang, Baiqing Yuan[*]

College of Chemistry and Chemical Engineering, Anyang Normal University, Anyang 455000, Henan, China
[*]E-mail: baiqingyuan1981@126.com

Nickel molybdate nanosheets were synthesized by a microwave-assisted solvothermal method, and the structure and morphology of the as-prepared nanosheets were characterized by powder X-ray diffraction (PXRD), transmission electron microscope (TEM), and high-resolution TEM (HRTEM). Serving as a non-enzymatic sensor, the $NiMoO_4$ nanosheet modified carbon paste electrode (CPE) demonstrated excellent electrocatalytic activity towards glucose oxidation with a high sensitivity and good stability. The results suggest that the $NiMoO_4$ nanosheet is a promising electrode material for enzyme-free glucose sensors.

Keywords: nickel molybdate; nanosheets; microwave-assisted solvothermal synthesis; glucose sensor

1. INTRODUCTION

Metal molybdates have received great attention for their widely using in many fields, such as catalysis [1, 2], photoluminescence [3], sensors [4], magnetic properties [5] and energy storage [6-11]. Nickel molybdate ($NiMoO_4$), an important metal molybdates, exhibits three distinct crystalline phases, namely, α-$NiMoO_4$, β-$NiMoO_4$, and the hydrate $NiMoO_4 \cdot nH_2O$ [7, 12]. The physical and chemical properties are closely related to the polymorph and shape. For example, the β-phase of $NiMoO_4$ presented twice of the selectivity for the dehydrogenation of propane to propene than the α-phase [13]. However, among these three polymorphs, β-$NiMoO_4$ is only stable at high temperature and will transit to α-phase when cooling down to room temperature [7, 12], which limit its application. It is significant to synthesize stable β-$NiMoO_4$ at room temperature. Recently, a mixed α-/β-$NiMoO_4$ film with mesoporous honeycomb structure was first produced through polymer templating, and the β-$NiMoO_4$ could be stabilized in the mesoporous film [7]. The shapes of $NiMoO_4$ are so far limited to rods [6, 9, 14], [15], particles [13, 16] and flowers [17], and the synthesis methods includes sol-gel [7],

impregnation [18], combustion [13], electrodeposition[17], and sonochemical method [15]. More recently, synthesis of ultrathin nanosheets materials are attracting more and more research interest due to their unique properties and applications [19-21]. However, $NiMoO_4$ nanosheets are not easily synthesized by common methods.

As a non-classical energy source, microwave dielectric heating exhibited many advantages of increasing product yields, and enhancing product purity or material properties over conventional heating method [22, 23]. Microwave-assisted method has been reported for the synthesis of barium tungstate nanosheets [24]. Recently, β-$NiMoO_4$ nanosheets which can be stabilized at room temperature were synthesized by a microwave-assisted solvothermal method [25]. However, to the best of our knowledge, the aplication of $NiMoO_4$ nanosheets in the enzyme-free glucose sensor has not been reported. Herein, the as-prepared $NiMoO_4$ nanosheets were first presented for the electrochemical detection of glucose. The results showed that the $NiMoO_4$ nanosheets exhibited high electrocatalytic activity towards the oxidation of glucose and good stability due to the strong interaction between the $NiMoO_4$ nanosheets and the electrode surface. In addition, the sensor showed low detection limit and wide linear range.

2. EXPERIMENTAL

2.1. Chemicals and solutions

$Ni(NO_3)_2 \cdot 6H_2O$, $Na_2MoO_4 \cdot 2H_2O$, glucose, uric acid (UA), ascorbic acid (AA), and dopamine (DA) were acquired from Sigma-Aldrichand used without further purified. All other chemicals used were of analytical reagent grade, and the aqueous solutions were prepared with doubly distilled water.

2.2. Apparatus

Scanning electron microscope (TEM) images were carried on a LEO1530. The resultant phase of the $NiMoO_4$ nanosheets was examined by X-ray diffraction (XRD, Cu Kα radiation, Rigaku D/max2550VB, Japan). Transmission electron microscope (TEM) images were performed with a HITACIA H7700 (Japan). HRTEM images were recorded on an FEI Tecnai G2 F20 s-twin D573. A CHI 842C electrochemical workstation (Austin, TX, USA) was used to carry out all the electrochemical experiments using $NiMoO_4$ modified carbon paste electrode ($NiMoO_4$-CPE) as working electrode, a platinum coil as auxiliary electrode, and a Ag/AgCl (saturated KCl) electrode as reference electrode.
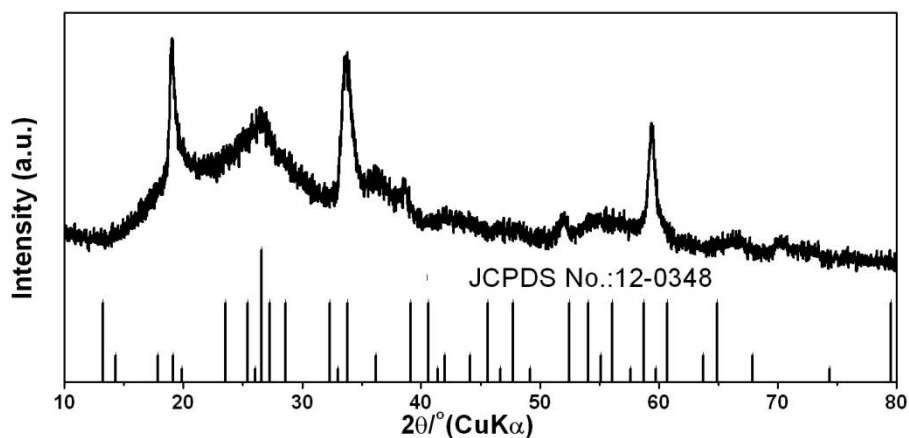
2.3. Preparation of NiMoO$_4$ nanosheets

$NiMoO_4$ nanosheets were synthesized according to previous report [25]. In brief, 0.23 g NaOH, 3.8 mL H_2O, 5.7 mL ethanol, and 2.3 mL oleic acid were mixed to form a reverse micelle system by stirring vigorously. 1.0 mL aqueous solution of $Ni(NO_3)_2 \cdot 6H_2O$ (0.2 mmol) was then added, the

mixture was stirred for a few minutes, and 1.0 mL of Na_2MoO_4 aqueous solution were added dropwise. After stirring for 20 min, all the mixture was transferred into a microwave glass vessel and irradiated for 10 min at 180 °C with a single-mode Microwave Synthesizer (Biotage AB, Sweden) and under magnetic stirring. The obtained products were separated by centrifugation and washed by ethanol and cyclohexane repeatedly, and finally redispersed in cyclohexane.

2.4. Fabrication of NiMoO₄-CPE

Bare CPE was prepared by mixing graphite powder and liquid paraffin with a ratio of 75:25 (w/w). A portion of the resulting paste was packed firmly into a glassy tube (1.8 mm inner diameter) by utilizing a copper wire to make electrical contact. NiMoO₄-CPE was fabricated by casting 5 µL 1 mg/mL NiMoO₄ suspension on the surface of bare CPE and the electrode was then dried in the atmosphere..
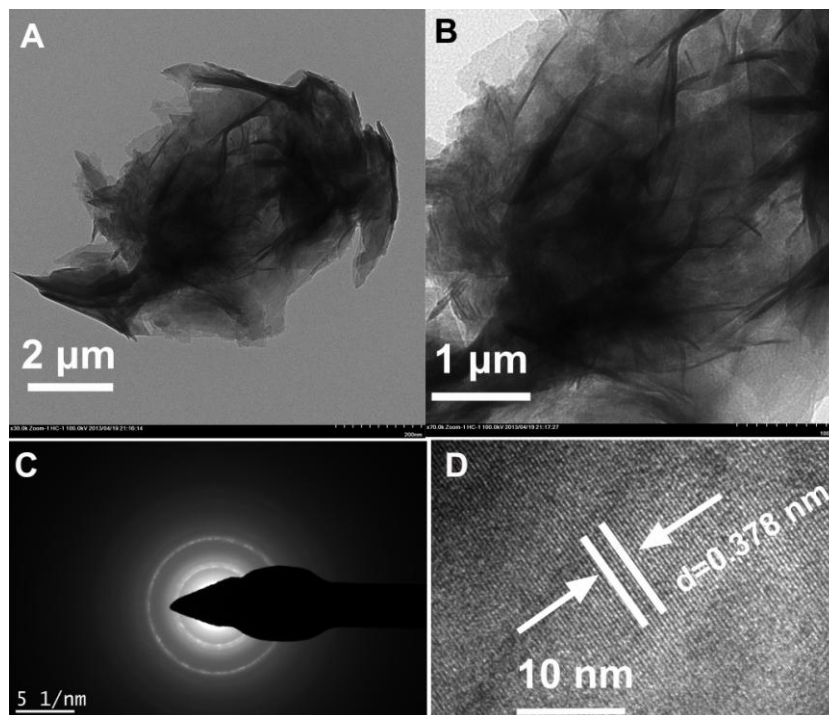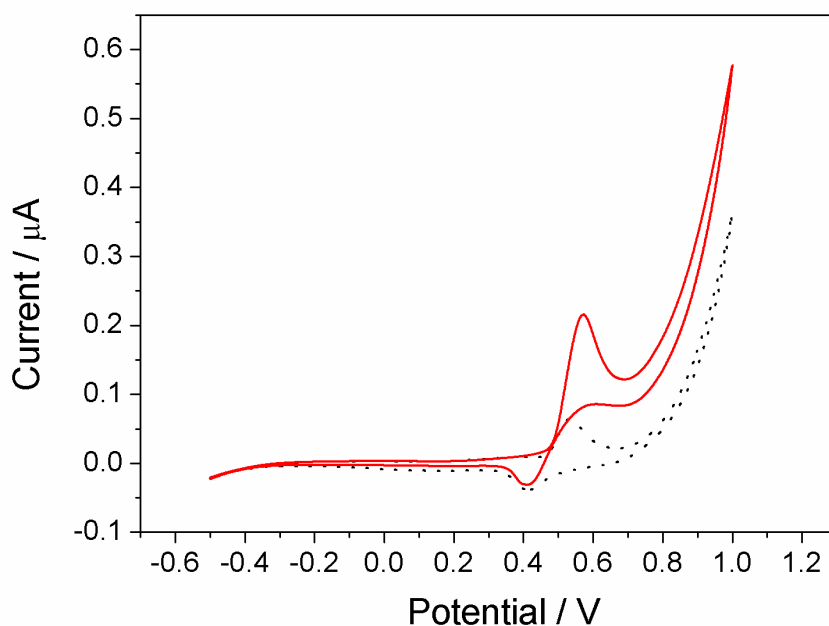
3. RESULTS AND DISCUSSION

Figure 1. XRD spectrum of the as-prepared NiMoO₄.

The crystalline structure of the as-obtained products is investigated by XRD (see Fig.1), which shows that the samples are of high crystallinity and the diffraction peaks in XRD can be indexed to the β-NiMoO₄ (JCPDS card no. 12-0348). Nickel oxide with the main reflections at 2θ=37.2° and 43.5° [12], frequently used for the stabilization of β-NiMoO₄, is not detected in the as-prepared products by XRD. Fig. 2 depicts the TEM and HRTEM images of the as-prepared products. The TEM image (Fig. 2A) indicates the product is a micrometer-size nanosheets. The morphology and structure of NiMoO₄ ultrathin nanosheets are further characterized by HRTEM (Fig.2C and D). The corresponding selected-area electron diffraction (SAED) pattern (Fig. 2C) indicates the polycrystalline nature of the products. The HRTEM image of a single NiMoO₄ nanosheet is shown in Fig.2D, highly ordered lattice fringes, even in the surface region, are evidence of the crystallinity of the nanosheets. The distance of lattice

finger is 0.378 nm, which is corresponding to the peak at 23.51 of β-NiMoO$_4$ phase. Previously literatures report that β-NiMoO$_4$ is only stable at high temperature and will transit to α-phase when cooling down to room temperature[12].
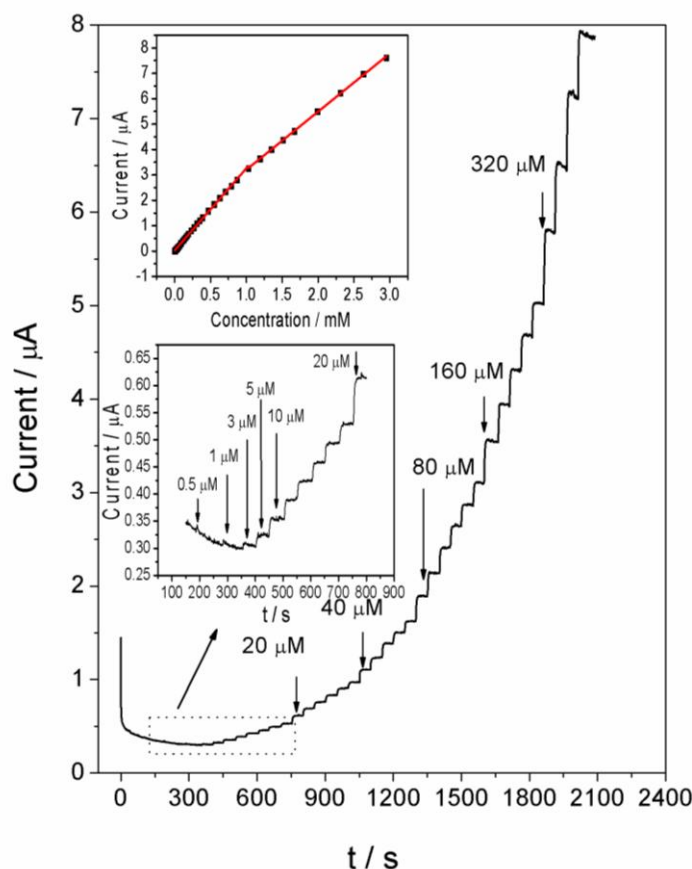

Figure 2. TEM images (A and B), SAED pattern (C), and HRTEM image (D) of β-NiMoO$_4$nanosheets.

Figure 3. CVs of NiMoO$_4$-CPE in the presence (solid line) and absence (dotted line) of 5 mM glucose in 0.1 M NaOH.

However, a mixed α-/β-NiMoO₄ film with mesoporous honeycomb structure was recently fabricated, and the β-NiMoO₄ could be stabilized in the mesoporous film at room temperature [7]. Therefore, we think that the large ultrathin structure might help to stabilize β-NiMoO₄ at room temperature.

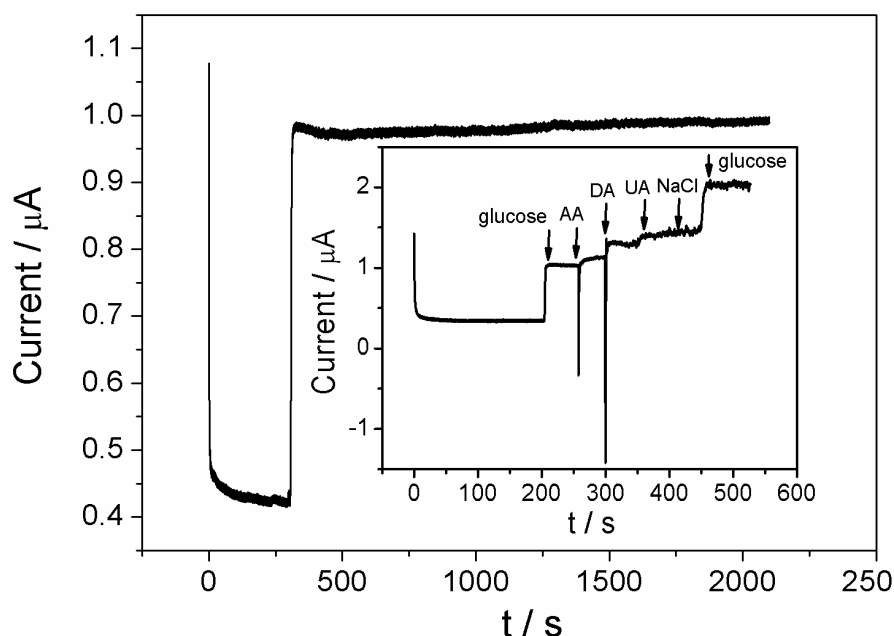The as-prepared β-NiMoO₄ can be firmly modified on the surface of carbon paste electrode (CPE) by a simple coating method, and the modified electrode was referred as NiMoO₄-CPE. Fig. 3 shows the CVs of NiMoO₄-CPE in the presence and absence of glucose in 0.1 M NaOH solution. As it can be seen, in the blank NaOH solution, the NiMoO₄-CPE exhibited a pair of redox peaks at 0.53 and 0.42 V, respectively, which was attributed to Ni(II)/Ni(III) redox couples formed in the alkaline medium. Upon addition of glucose, notable enhancement of the anodic current was observed, suggesting that the NiMoO₄-CPE catalyzed the oxidation of glucose.

Figure 4. Amperometric sensing of glucose by successive addition of glucose at NiMoO₄-CPE at 0.6 V in 0.1 M NaOH. Inset, plot of amperometric response versus the concentration of glucose from 3 µM to 1.03 mM and 1.03 to 2.95 mM, respectively.

The amperometric responses to successive additions of glucose at the NiMoO₄-CPE are shown in Fig. 4. When glucose was injected to the electrochemical cell, a rapid increase in the oxidation current was observed and reached the steady-state current with 5 s. As shown in the inset of Fig. 4, the calibration curves for glucose detection are linear from 3 µM to 1.03 mM (R=0.9984) and 1.03 to 2.95

mM (R=0.9995) with the detection limit of 1 μM. The detection repeatability of a $NiMoO_4$-CPE was estimated from five successive measurements of 20 μM glucose, and the relative standard deviation (RSD) was 3.9%. In order to evaluate the stability of the sensor, long-term amperometric response to 0.25 mM glucose was examined (shown in Fig. 5). The amperometric response remains at 99% of the initial current after 2000 s of continuous operating, indicating excellent stability of the presented electrode. The strong interaction between $NiMoO_4$ and graphite might be formed due to the large ultrathin structure of $NiMoO_4$ nanosheets, which may explain the good stability of $NiMoO_4$-CPE. The influence of various foreign species including ascorbic acid (AA), dopamine (DA), uric acid (UA), and NaCl was also investigated (Fig. 5). The results showed that 0.02 mM AA, 0.02 mM DA, 0.02 mM UA, and 0.3 mM NaCl did not affect significantly the determination of 0.3 mM glucose. In addition, as shown in Fig. 4, the amperometric responses to 0.3 mM glucose almost kept constant before and after these foreign species were added, revealing high anti-interference ability and stability of the $NiMoO_4$-CPE. In order to demonstrate the practical use of the proposed sensor, the sensor was presented for the analysis of glucose spiked in human urine by standard addition method. The measured concentration was in good agreement with the value obtained by commercial glucose meter, and the recovery rate was between 97% and 104%.

Figure 5. Long-term amperometric test of $NiMoO_4$-CPE with 0.25 mM glucose. Inset, interference test of $NiMoO_4$-CPE with 0.3 mM glucose in the presence of 0.02 mM AA, 0.02 mM DA, 0.02 mM UA, and 0.3 mMNaCl.

4. CONCLUSIONS

In summary, large β-$NiMoO_4$ nanosheets were prepared by a simple microwave-assisted solvothermal method, which is stable at room temperature. The as-prepared β-$NiMoO_4$ nanosheets

exhibited high electrocatalytic activity towards the oxidation of glucose, and a novel enzyme-free glucose sensor was fabricated accordingly. The special ultrathin structure of β-NiMoO₄ nanosheets may play an important role in the stability of both β-NiMoO₄ and the presented sensor. With the growing research interests for two-dimensional ultrathin nanosheets, it will be significant and possible to synthesize novel NiMoO₄ composites with other 2D materials like graphene or graphene analogues.

References

1 G. J. Jin, W. H. Weng, Z. J. Lin, N. F. Dummer, S. H. Taylor, C. J. Kiely, J. K. Bartley and G. J. Hutchings, *J. Catal.*, 296 (2012) 55.
2 D. L. Stern and R. K. Grasselli, *J. Catal.*, 167 (1997) 550.
3 W. S. Wang, L. Zhen, C. Y. Xu and W. Z. Shao, Cryst. *Growth Des.*, 9 (2009) 1558.
4 Q. Dai, G. Zhang, P. Liu, J. Wang and J. Tang, *Inorg. Chem.*, 51 (2012) 9232.
5 Y. Ding, S.H. Yu, C. Liu and Z.A. Zang, *Chem. Eur. J.*, 13 (2007) 746.
6 W. Xiao, J. S. Chen, C. M. Li, R. Xu and X. W. Lou, *Chem. Mater.*, 22 (2010) 746.
7 J. Haetge, I. Djerdj and T. Brezesinski, *Chem. Commun.*, 48 (2012) 6726.
8 B. Senthilkumar, D. Meyrick, Y. S. Lee, Ramakrishnan and K. Selvan, *RSC Adv.*, 3 (2013) 16542.
9 Z. X. Yin, S. Zhang, Y. J. Chen, P.Gao, C. L. Zhu,P. P. Yang and L. H. Qi, *J. Mater. Chem. A*, 3 (2015) 739.
10 M. C. Liu, L. B. Kong, X. J. Ma, C. Lu, X. M. Li, Y. C. Luo and L. Kang, *New J. Chem.,* 36 (2012) 1713.
11 Q. Sun, Q. Q. Ren and Z. W. Fu, *Electrochem. Commun.*, 23 (2012) 145.
12 B. Moreno, E. Chinarro, M. T. Colomer and J. R. Jurado, *J. Phys. Chem. C*, 114 (2010) 4251–4257.
13 C. Mazzocchia, C. Aboumrad, C. Diagne, E. Tempesti, J. M. Herrmann and G. Thomas, *Catal. Lett.*, 10 (1991) 181.
14 Y. Ding, Y. Wan, Y. L. Min, W. Zhang and S. H. Yu, *Inorg. Chem.* 47 (2008) 7813.
15 G. Kianpour, M. Salavati-Niasari and H. Emadi, *Ultrason. Sonochem.*, 20 (2013) 418.
16 B. Senthilkumar, K. V. Sankar, R. K. Selvan, M. Danielle and M. Manickam, *RSC Adv.*, 3 (2013) 352.
17 U. Lačnjevac, B. M. Jović, Z. Baščarević, V. M. Maksimović and V. D. Jović, *Electrochim. Acta*, 54 (2009) 3115.
18 U. Ozkan and G. L. Schrader, *J. Catal.*, 95 (1985)137.
19 C. Z. Wu, X. L. Lu, L. L. Peng, K. Xu, X. Peng, J. L. Huang, G. H. Yu and Y. Xie, *Nature commun.*, 4 (2013) 2431.
20 H. Hwang, H. Kim and J. Cho, *Nano Lett.*, 11 (2011) 4826.
21 J. Q. Tian, Q. Liu, A. M. Asiri, A. O. Al-Youbi and X. P. Sun, *Anal. Chem.*, 85 (2013)5595.
22 M. Baghbanzadeh, L. Carbone, P. D. Cozzoli and C. O. Kappe, *Angew. Chem. Int. Ed.*, 50 (2011)11312.
23 I. Bilecka and M. Niederberger, *Nanoscale*, 2 (2010) 1358.
24 Z. J. Luo, H. M. Li, J. X. Xia, W. S. Zhu, J. X. Guo, B. B. Zhang, *Mater. Lett.*, 61 (2007)1845.

3159

25 D. J. Zhang, R. C. Zhang, C. Y.Xu, Y. Fan, B. Q. Yuan, *Sensors and Actuators B,* 206 (2015) 1.